Supplementary Material

High piezoelectricity of Eu^{3+}-doped $Pb(Mg_{1/3}Nb_{2/3})O_3$-$0.25PbTiO_3$ transparent ceramics

Kai Li[1], Enwei Sun[1,*], Yongcheng Zhang[2,*], Zhenzhen Song[2], Xudong Qi[1], Yuan Sun[1], Jiaming Li[1], Bin Yang[1,*], Jian Liu[1], Wenwu Cao[1,3]

[1]*Condensed Matter Science and Technology Institute, School of Instrumentation Science and Engineering, Harbin Institute of Technology, Harbin 150080, China*

[2]*College of Physics and University-Industry Joint Center for Ocean Observation and Broadband Communication, Qingdao University, Qingdao 266071, China*

[3]*Department of Mathematics and Materials Research Institute, The Pennsylvania State University, University Park, Pennsylvania 16802, USA*

*Corresponding authors. *E-mail addresses*: sunew@hit.edu.cn (E. Sun), qdzhyc@qdu.edu.cn (Y. Zhang), binyang@hit.edu.cn (B. Yang)

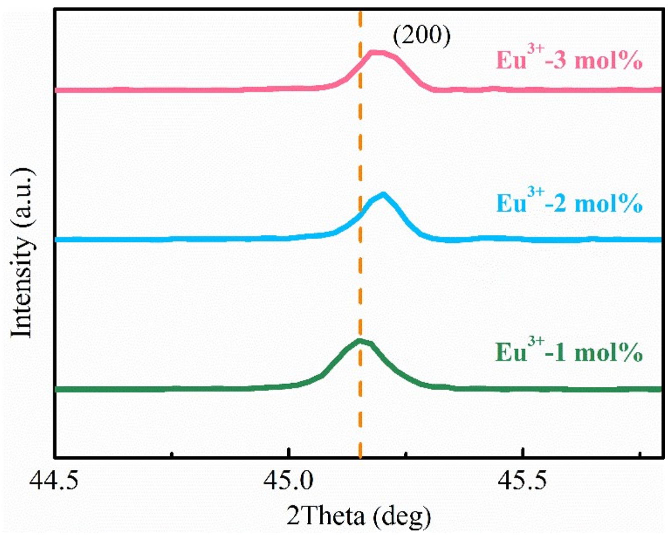

Fig. S1. The enlarged XRD patterns of Eu^{3+} doped PMN-PT transparent ceramics with the 2θ ranging from 44.5° to 45.8°.

The Vogel-Fulcher (V-F) relation is given by[1,2]:

$$f = f_0 \exp[\frac{-E_a}{k(T_\mathrm{m} - T_f)}] \quad \text{(S1)}$$

where f_0, f, T_m and k are the Debye frequency, measurement frequency, temperature corresponding to the maximum dielectric constant, and the Boltzmann constant. The E_a and T_f are the activation energy of local polarization and static freezing temperature of the thermal activation behavior of electric dipoles, i.e., the transition temperature between macro-domain and micro-domain structures. For ralaxor ferroelectrics, when the temperature is above T_f, macro-domains disappear while polar nanoregions develop. When temperature is below T_f the polar nanoregion dynamics will be frozen and the system will be in the low-temperature ferroelectric (FE) phase. In PMN-0.25PT:Eu^{3+} ceramics, the relationship between T_m and f was fitted by Eq. (S1), as seen in Fig. S2 (a)-(c). The corresponding parameters are obtained and listed in Table S1.

In addition, the dielectric quadratic relation is suggested as follows[3]:

$$\frac{\varepsilon_\mathrm{A}}{\varepsilon} - 1 = \frac{(T - T_\mathrm{A})^2}{2\delta^2} \quad \text{(S2)}$$

where the value of the fitting δ parameter represents the diffuse degree of phase transition. Fig. S2(d)-(f) illustrate the temperature and frequency dependence of dielectric permittivity and the fitting using Eq. (S2) for PMN-0.25PT:Eu^{3+} ceramics. Obviously, the experimental data were fitted well and the parameters were listed in Table S1. Furthermore, the ΔT_m (ΔT_m = T_m (100 kHz)-T_m (100 Hz)) was also calculated and listed in Table S1. We can see that the degree of dielectric relaxation is stronger for higher Eu^{3+} doping amount.

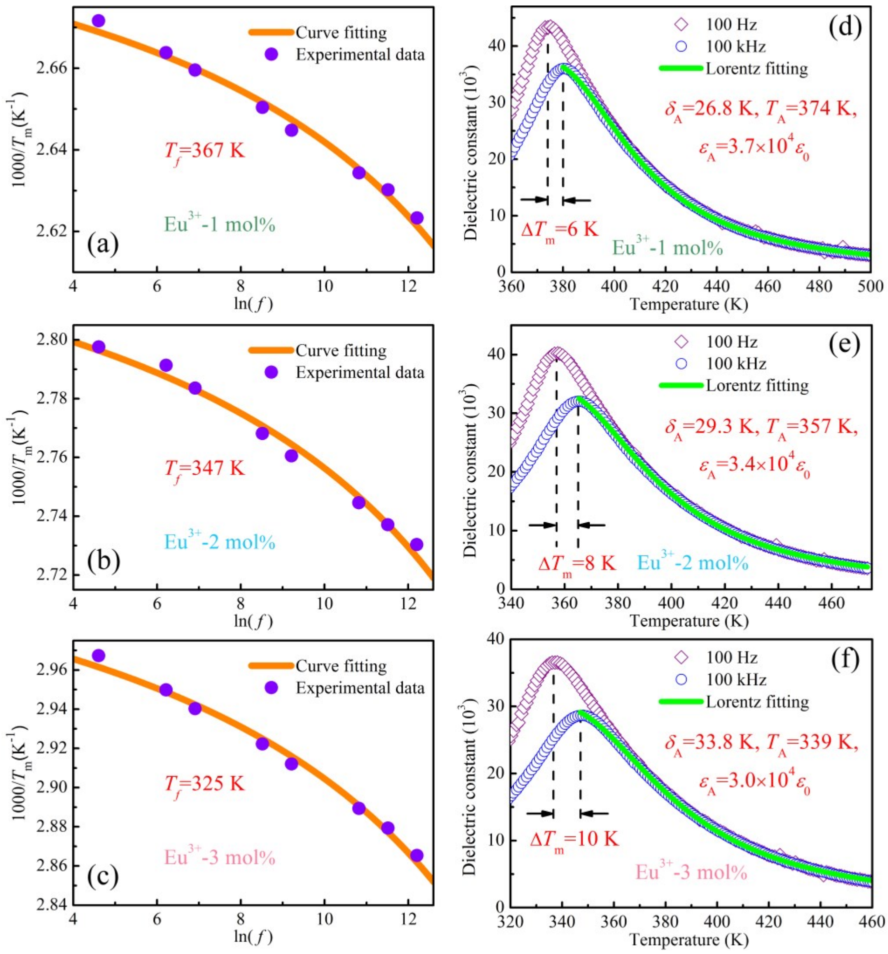

Fig. S2. The Vogel-Fulcher law and Lorentz-type relation fitting results for PMN-0.25PT:Eu^{3+} ceramics, (a), (d) 1 mol% Eu^{3+}, (b), (e) 2 mol% Eu^{3+} and (c), (f) 3 mol% Eu^{3+}.

Table S1 The values of ΔT_m and fitting parameters for Eu^{3+}-doped PMN-0.25PT ceramics.

Eu^{3+} (mol%)	f_0 (10^5 kHz)	E_a/k (K)	T_f (K)	ΔT_m (K)	δ (K)	T_A (K)	ε_A ($10^3\varepsilon_0$)
1	9.6	122	367	6	26.8	374	37
2	9.8	166	347	8	29.3	357	34
3	10	212	325	10	33.8	339	30

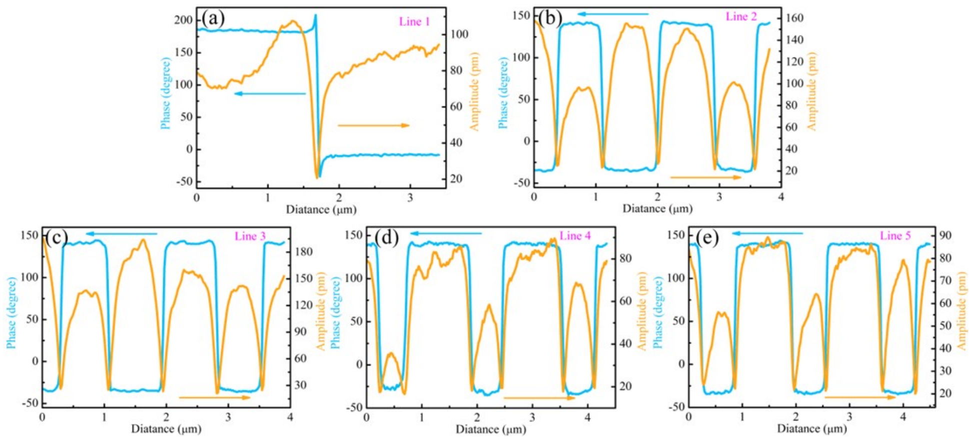

Fig. S3. The piezoresponse amplitude and phase degree of the line scanning across the domain patterns of 2mol% Eu^{3+}-doped PMN-0.25PT transparent ceramics.

The piezoelectric coefficients (d_{33}) of various transparent ferroelectric ceramics shown in Fig.4 were taken from ref. 4-18.

References

1 S. M. Gupta and D. Viehland, *J. Am. Ceram. Soc.*, 1997, **80**, 477−485.

2 X. D. Qi, Y. Zhao, E. W. Sun, J. Du, K. Li, Y. Sun, B. Yang, R. Zhang and W. W. Cao, *J. Eur. Ceram. Soc.*, 2019, **39**, 4060−4069.

3 T. Zheng, L. H. Luo, P. Du, A. M. Deng and W. P. Li, *J. Eur. Ceram. Soc.*, 2017, 38, 575−583.

4 I. Fujii, S. Nakashima and T. Wada, *J. Am. Ceram. Soc.*, 2019, **102**, 1240−1248.

5 K. Yan, X. L. Chen, F. F. Wang and K. J. Zhu, *Appl. Phys. Lett.*, 2020, **116**, 082902.

6 K. B. Chu, Y. Shi, K. Li, B. J. Fang and J. J. Ding, *J. Phys. Chem. Solids.*, 2015, **81**, 10−14.

7 B. K. Wang, X. X. Tian, Z. Xu, S. B. Qu and Z. R. Li, *Acta. Phys. Sin-ch Ed.*,

2012, **19**, 197703.

8 J. F. Lin, J. Xu, C. W. Liu, Y. H. Lin, X. Wu, C. Lin, X. H. Zheng and C. Chen, *J. Alloy. Comp.*, 2019, **784**, 60−67.

9 A. Rahmana, S. Parka, Y. Mina, G. T. Hwanga, J. J. Choia, B. D. Hahna, K. H. Chob, S. Nahmd and C. W. Ahna, *J. Eur. Ceram. Soc.*, 2020, **40**, 2989−2995.

10 X. S. Zhang, D. Yang, Z. Y. Yang, X. M. Zhao, Q. Z. Chai, X. L. Chao, L. L. Wei and Z. P. Yang. *Ceram. Int.*, 2016, **42**, 17963−17971.

11 Z. M. Geng, K. Li, D. L. Shi, L. L. Zhang and X. Y. Shi, *J. Mater. Sci-Mater. El.*, 2015, **26**, 6769−6775.

12 D. Yang, C. Ma, Z. P. Yang. L. L. Wei, X. L. Chao, Z. Y. Yang and J. L. Yang, *Ceram. Int.*, 2016, **42**, 4648−4657.

13 C. Huang, J. M. Xu, Z. Fang, D. Ai, W. Zhou, L. Zhao, J. Sun and Q. Wang, *J. Alloy. Comp.*, 2017, **723**, 602−610.

14 X. D. Ren, Z. H. Peng, B. Chen, Q. Q. Shi, X. S. Qiao, D. Wu, G. R. Li, L. Jin, Z. P. Yang and X. L. Chao, *J. Eur. Ceram. Soc.*, 2020, **40**, 2331−2337.

15 X. M. Zhao, Q. Z. Chai, B. Chen, X. L. Chao and Z. P. Yang. *J. Am. Ceram. Soc.*, 2018, **101**, 5127−5137.

16 S. Y. Cao, F. Gao, J. Xu, J. H. Zhu, Q. Chen, Y. T. Guo, L. L. Li, J. T. Liu, T. Gao, E. Pawlikowska, M. Szafran and G. H. Cheng, *J. Eur. Ceram. Soc.*, 2019, **39**, 5260−5266.

17 X. Wu, C. C. Fang, J. F. Lin, C. W. Liu, L. H. Luo, M. Lin, X. H. Zheng and C. Lin, *Ceram. Int.*, 2018, **44**, 4908−4914.

18 X. M. Zhao, X. L. Chao, D. Wu, P. F. Liang and Z. P. Yang, *J. Am. Ceram. Soc.* 2019, **102**, 3498−3509.